Tubular microfossils from 2.8 to 2.7Ga-old lacustrine deposits of South Africa: A sign for early origin of eukaryotes?

Journal Item

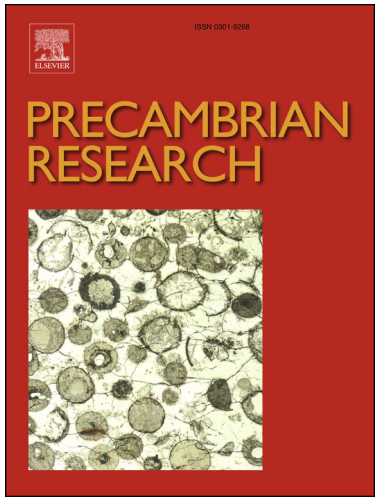

Tubular microfossils from ~2.8 – 2.7 Ga-old lacustrine deposits of South Africa: a sign for early origin of eukaryotes?

Józef Kaźmierczak, Barbara Kremer, Wladyslaw Altermann, Ian Franchi

PII: S0301-9268(16)30140-1
DOI: http://dx.doi.org/10.1016/j.precamres.2016.10.001
Reference: PRECAM 4593

To appear in: *Precambrian Research*

Received Date: 13 May 2016
Revised Date: 26 September 2016
Accepted Date: 2 October 2016

Please cite this article as: J. Kaźmierczak, B. Kremer, W. Altermann, I. Franchi, Tubular microfossils from ~2.8 – 2.7 Ga-old lacustrine deposits of South Africa: a sign for early origin of eukaryotes?, *Precambrian Research* (2016), doi: http://dx.doi.org/10.1016/j.precamres.2016.10.001

Tubular microfossils from ~2.8 – 2.7 Ga-old lacustrine deposits of South Africa: a sign for early origin of eukaryotes?

Józef Kaźmierczak[a*] Barbara Kremer[a], Wladyslaw Altermann[b], Ian Franchi[c]

[a]Institute of Paleobiology, Polish Academy of Sciences, Twarda 51/55, 00-818 Warsaw, Poland,

[b]Kumba-Exxaro Chair, Department of Geology, University of Pretoria, Republic of South Africa,

[c]Planetary and Space Sciences, Open University, Milton Keynes, MK7 6AA, United Kingdom.

*Corresponding author at: Institute of Paleobiology, Polish Academy of Sciences, Twarda 51/55, 00-818 Warsaw, Poland,

E-mail: jkaz@twarda.pan.pl.

ABSTRACT

Unequivocal evidence for Archean eukaryotic life has been long sought for and is a matter of lively debate. In the absence of unambiguous fossils this debate has focused on biogeochemical signatures and molecular phylogenies. Most researchers agree that fossil forms comparable with modern eukaryotic cells can be credibly identified only in Proterozoic (~1.8-1.6 Ga) and younger rocks. Herein, we report for the first time, Neoarchean mineralized tubular microfossils from ~2.8-2.7 Ga lacustrine deposits of South Africa. The exceptional preservation of these microfossils allows recognition of important morphological details in petrographic thin section and in HF-macerates that links them to modern siphonous (coenocytic) green or yellow-green microalgae (Chlorophyta and Xanthophyta). The microfossil identification is supported by Raman spectroscopic analyses, EPMA, SEM/BSE

and SEM/EDS microprobe analytical results, NanoSIMS elemental mapping and micro-tomographic sectioning of the thalli. All results point to indigenous, bona fide eukaryotic microfossils of algal affinity. These Neoarchean microalgae-like remains and their assumingly combined *in vivo* and early post-mortem precipitated mineral envelopes greatly improve our knowledge of early life and its habitats and may have far-reaching consequences for the studies of the evolution of life.

1. Introduction

The presence of Archean prokaryotic life, including photosynthesizing cyanobacteria, is almost uniformly accepted today (for review see: Awramik, 1992; Nisbet and Sleep, 2001; Altermann and Kazmierczak, 2003; Brasier et al., 2006; Schopf et al., 2007; Knoll, 2015). Evidence of eukaryotic life in the Archean remains elusive. Thus far, the claims or suggestions for Archean eukaryotes based on hydrocarbon biomarkers or morphological objects (Waldbauer et al., 2009; Javaux et al., 2010; Buick, 2010) have been repudiated or remain inconclusive (Rasmussen et al., 2008; Knoll, 2014; French et al., 2015).

Information on the time of appearance of eukaryotic life may be provided by molecular phylogeny although the confidence placed in the results of molecular clock modelling is far from commonly accepted (e.g., Pulquério and Nichols, 2007; Yoder, 2013). Attempts to establish a time-scale of eukaryote evolution based on molecular phylogeny have led indeed to contradictory results: from not earlier as 1100 Myr to as old as 3970 Myr (e.g., Dickerson, 1971; Feng et al., 1997; Hedges et al., 2001, 2004; Douzery et al., 2004; Roger & Hug, 2011). These estimations were recently reviewed (Eme et al., 2014), restudied and constrained using taxon-rich multigene data and a relaxed molecular clock framework (Parfrey et al., 2011). Accordingly, the time of the last common ancestor of modern eukaryotes (including longer stems preceding the diversification in the major eukaryotic lineages) has been evaluated at

between 1.866 and 1.679 Ga. It is widely accepted that this is in congruency with the fossil record which documents relatively diversified remnants of credible eukaryotic microfossils starting from ~1.8 Ga ago (Knoll et al., 2006). Below, based on rich and well-preserved cellular remnants of 2.8-2.7 Ga-old tabular microfossils from South Africa, reminiscent of modern and geologically much younger siphonous microalgae, we argue that these opinions may however be significantly changed.

2. Materials and methods

2.1. Sample description

The study is based on three samples, each weighing about 0.5kg, labeled SA-31, SA2-215, and SA2-178, collected during two field campaigns (2007 and 2010) in a natural outcrop of the c. 2739 Ma Omdraaivlei Fm. (Sodium Group, Ventersdorp Supergroup; Altermann and Lenhardt, 2012) located on Kaapvaal Craton between Britstown and Prieska (sampling coordinates: 30˚02'56.0''S; 23˚10'24.3''E).

2.2. HF rock samples maceration

Small (15x15x15 mm) cubes of rock samples SA-31 and SA2-178 were macerated for traces of organic materials with 40% hydrofluoric acid (HF). The cubes were treated with HF in 12 and 24 hours trials. The macerated fragments of thalli were, after decantation, mounted with pipette on concavity slides, covered with coverslips, and examined in transmitted light with optical microscope.

2.3. Light microscopy

Standard microscopic analyses with a Zeiss-Opton light microscope were performed on over hundred of specimens of the tubular microfossils observed in 15 covered and uncovered

polished petrographic thin sections. Because glass cover reduces effect of light scattering, covered petrographic thin sections were used for getting high quality light microscope images.

2.4. SEM and EDS

The scanning electron microscope SEM examination involved a Philips XL 20 instrument, equipped with an EDX dual-window (UTW/Open) microprobe equipped in turn with an ECON detector model Econ-6 (Institute of Paleobiology, Polish Academy of Sciences, Warsaw). Rock platelets for scanning electron microscopic (SEM) examinations were polished and etched for a few minutes with 40% hydrofluoric acid. Some macerated specimens after dehydration were mounted on copper table, sputtered with platinum and analyzed with Energy Dispersive Spectroscopy on SEM (SEM-EDS).

2.5. EPMA

Cameca SX-100 electron microprobe analyses (EPMA) were performed at the Joint-Institute Analytical Complex for Minerals and Synthetic Substance (University of Warsaw).

2.6. Raman

Micro-Raman measurements were performed at the Laboratory of Intermolecular Interactions, Faculty of Chemistry, Warsaw University. Point mapping was performed with a LabRAM HR800 (Horiba Jobin Yvon) spectrometer, coupled with an Olympus BX61 confocal microscope. The laser spot size was about 500 nm.

2.7. NanoSIMS

NanoSIMS analyses were performed with the Cameca NanoSIMS 50L at Planetary and Space Sciences of the Open University (Milton Keynes, UK). The samples were pre-sputtered over an area of approx. 25 x 25 µm for approximately 1 hour to remove surface contamination.

Analyses were performed over approximately 20 x 20 µm areas, with a 50pA Cs^+ probe and the electron gun used for charge compensation. The analysis of each area lasted 2-4 hours and comprised multiple scans of the area. The instrument was set up with a mass resolving power of more than 8000 (Cameca NanoSIMS definition) and ^{12}C, $^{12}C^{14}N$, ^{28}Si, ^{32}S, $^{27}Al^{16}O$ and $^{40}Ca^{16}O$ collected on electron multiplers simultaneously. The large primary probe offered useful count rates of ^{12}C, $^{12}C^{14}N$ and ^{32}S, although the probe size limited spatial resolution to approximately 500 nm.

2.8. Mineralogical Analysis

The phase composition of the samples was identified at the Institute of Geological Sciences PAS (Warsaw) by powder X-ray diffraction using powder diffractometer Bruker axs D8 Advance Serie 2 with position sensitive detector Vantec-1. Analysis parameters: Co lamp with Kα radiation, Kβ filter (Fe); generator setting: 35kV, 40 mA; angle range: 3–80 2θ degrees; scan step: 0,0218 2θ degrees; scan speed: 1 s/step. DIFFRACplus Evaluation package (EVA) version 11.0 software was used to process the data.

2.9. Micro-computed tomography

Micro-CT data were collected with Zeiss XRadia MicroXCT-200 imaging system equipped with a 90 kV/8W tungsten X-ray source in the Laboratory of Microtomography, Institute of Paleobiology, Polish Academy of Science, Warsaw. Scans were performed using the following parameters: voltage: 50kV, power: 6W, 1201 projections per sample, exposure time: 100s, voxel size: 1,03 µm. Radial projections were reconstructed with XMReconstructor software. The serial micro-CT sections were obtained with XM3DViewer software.

3. Geographic and geological location

The 2.8-2.7 Ga Sodium Group, from which the tubular microfossils described herein were derived, is a volcano-sedimentary succession correlated with the Neoarchean Ventersdorp Supergroup (Kaapvaal Craton, South Africa; Fig. 1A) (Grobler et al., 1989; Buck, 1980; Altermann and Lenhardt, 2012). Coccoidal, bacteria-like microfossils and stromatolites were previously described from the Sodium Group and the Ventersdorp Supergroup (Buck, 1980; van der Westhuizen et al., 1991; Altermann and Lenhardt, 2012). The lacustrine deposits in which the eukaryote-like microfossils were found belong to the 2.74-2.71 Ga Omdraaivlei Formation (Altermann and Lenhardt, 2012), where nine carbonate intervals occur in tuffaceous shale (Fig. 1B), as beds and lenses of stratiform and pseudocolumnar stromatolites (stratiform to laterally linked, hemispheroidal, narrow columns) (Fig. 2A). The stromatolitic carbonate beds (lithostromes) are commonly topped by symmetrical or asymmetrical ripples (Fig. 2B), preserved probably due to microbial mat overgrowth that stabilized the fine volcaniclastic sediment (Altermann and Lenhardt, 2012). In some stromatolitic beds, laterally linked columns are uniformly inclined and, together with the rippled stromatolite tops, indicate current action. Thinner beds of domical and stratiform stromatolites formed in a similar but less agitated, low energy shallow lacustrine environment (Buck, 1980; Altermann, 2007; Altermann and Lenhardt, 2012). Above the uppermost stromatolitic bed, sedimentation continued with shale and tuffacoeus sandstone intercalations, covered by lava flows. The carbonate beds are strongly silicified and recrystallization of chert and carbonate is common. Partial early diagenetic silicification is expressed by diagenetic silica, visible as minute quartz crystallites mixed with fine carbonaceous flakes (kerogen) within the laminae. Subsequently, SiO_2 has recrystallized to coarser, clean chert, with carbonaceous material squeezed between the chert crystallites of c. 10 µm diameter. Nevertheless, organo-sedimentary structures like laminae and tufts are very well preserved (Fig. 2C).

4. The tubular microfossils: distribution, morphology, composition

The tubular microfossils discussed herein occur with varying frequency in all stromatolitic intervals of the studied section. They are particularly abundant in the main stromatolitic unit (bed 11) indicated on Fig. 1B with a red arrow head. This c. 90 cm thick microbialitic bed is composed of strongly silicified narrow columns inclined in places towards the current, and of wavy laminites, both intercalating with each other and exhibiting rippled surfaces as described above.

The best-preserved microfossil specimens occur as dichotomously and trichotomously branched, mineralized tubes, up to several hundred micrometers long and 20 to 70 µm in diameter (Fig. 2D-F). Ten well branched specimens were found in petrographic thin-sections (Fig. 3A-E) and several in micro-tomographic sections (Fig. 3F-K; Suppl. Movie) (samples: SA-31, SA2-178). Hundreds of smaller fragments of such tubular structures were observed randomly distributed in the tuffaceous interlayers and clumpy fine sediment inclusions, typically as straight to slightly sinuous, stick-like mineralized tubes (Figs. 2D-F, 4). The mineral walls of the tubes are 10 to 20 µm thick, characteristically composed of coarse silicate minerals, mostly chunky, but often divided into equant or individual blocky crystallites (Fig. 4). The external surfaces of the tubes are irregular and rough whereas their internal surfaces are smooth. The lumen of the tubes is in most specimens filled with a kerogenous-mineralic substance of flaky to microgranular appearance, which in transparent longitudinal sections is visible as continuous brownish strand (or band). These strands range from thick, filling almost entirely the tube space (Figs. 2E, F), to thinner, occupying, often discontinuously, no more than half of the tube (Fig. 4B). When the strands are absent, the tubes are filled with translucent chert (Fig. 4A). The jagged ends of the tube fragments indicate that they are parts of mechanically broken, longer tubular structures (Figs. 2F, 5A).

Chemical and spectral analyses of the tubular structures by EPMA, NanoSIMS and SEM/EDS (Figs. 5-7) revealed the presence of two kinds of aluminosilicates: (i) Al-K-Fe-Mg silicate forming the walls of the tubes, and (ii) Al-Fe-Mg silicate comprising the continuous brownish bands in the tube interiors. Bulk X-ray diffractometry of the cherty sediment enclosing the tubular microfossils (Fig. 8) confronted with the EPMA and SEM/EDS elemental composition of the tubes (Figs. 5-7) indicate chamosite forming the mineral walls and muscovite-2M1 the internal strands. The element totals determined by EPMA are always below 100% for these samples, suggesting the presence of light elements in the tubular structures: about 2% in the tube walls and almost 10% in the brownish internal strands. NanoSIMS and micro-Raman analyses show the presence of particulate organic carbon in both cases (Fig. 5). In addition to C, NanoSIMS analyses confirmed the presence of S and N, both in the tube walls and in the brownish internal strands, indicating their biogenicity. Typical biogenic signatures were also obtained from $^{12}C/^{14}N$ ratios (comp. Schopf et al., 2007; Oehler et al., 2010).

The tubes and their carbon-rich internal bands lack cross walls, constrictions or other signs of septation or compartmentalization. After brief etching of the polished longitudinal sections with 40% HF, the tube walls exposed numerous small spheroid and rod- shaped, bacteria-like bodies in SEM images (Fig. 9A, B). Elemental electron dispersive spectra (SEM-EDS) of these bodies showed enrichment in Si and Ti, in contrast to the Ti-free Al-K-Mg-Fe silicate material building the bulk of the tube mineral walls (Fig. 9C, D). Micro-Raman spectra suggest a mixture of anatase and rutile as mineral components of the Ti-enriched bodies (Fig. 9E).

5. Comparison with modern and younger analogs

5.1. Arguments for siphonalean microalgae as analogs

The continuous carbon-rich strands (bands) inside most specimens examined can be interpreted as remains of variously shrunken cell content. They suggest similarity of these Neoarchean microfossils to coenocytic life forms known in diverse and unrelated groups of algae (green, yellow-green, red) and fungi. In the simplest modern case, a coenocytic construct is a multinucleate single giant tubular cell (called siphon) lacking cross walls (Kaplan and Hagemann, 1991; Niklas, 2000; Graham et al., 2009). Hence the adjective 'siphonous' used for such thallus organization. More advanced 'siphonous' forms (some red algae and fungal mycelia) are differently as the continuously open Omdraaivlei tubes characterized by multicellular thalli composed of coenocytic cells. In typical siphonous algae, in which nuclei are not organized in regularly spaced cytoplasm units, the cytoplasm exhibits streaming enabling transportation of organelles and nutrients across the thallus. The densely packed epiparietal chloroplasts are discoid or united in a reticulum. Both non-calcifying and calcifying representatives are known in modern siphonous algae, ranging in size between tens of micrometers to several meters in length (Vroom and Smith, 2003).

In most siphonous species the tubular central (axial) stipe is branched and the arrangement of the branches is used to describe their anatomical complexity and as taxonomic traits. The mode of branching of the Omdraaivlei tubular microfossils, with terminally located distinct branches of first and second order make them similar to modern representatives of siphonous green algae (Ulvophyta) classified to the order Bryopsidales (Figs. 3L, M; 10G, 12A) and to members of yellow-green algae (Xanthophyta) of the order Vaucheriales. The latter are known for their common extremely heavy calcification of thalli (Freytet and Verrecchia, 1998; Golubic et al., 2008; Gradziński, 2010). Vaucheriacean algae are typically inhabitants of hard water lakes and fluvial waters, although brackish and marine forms are also known (Graham et al., 2009). Since all the tubular Omdraaivlei fossils are fragmented, we can only

assume from their morphological similarity to these modern siphonous microalgae that they occurred as tiny brush- or bush-like turf adhered to the substratum by a system of rhizoids.

The sparse dichotomous and trichotomous branching of the Omdraaivlei microalgae (Figs. 3A-E; 12B, C) makes them particularly similar to the branching mode of thalli characteristic of modern species of the order Bryopsidales such as *Chlorodesmis* (Ducker, 1967), *Rhipilia* (Verbruggen and Schils, 2012) and particularly *Pseudochlorodesmis* and *Bryopsis* (Børgesen, 1925) (Fig. 3L, M). The diminutive siphon of *Pseudochlorodesmis*, if branched at all, does so only a few times (Fig. 3L). With the exception of some constrictions occurring only close the ramified rhizoids, the 70 µm thick cylindrical thalli of *Pseudochlorodesmis* are without constrictions through their whole length. Such simple sparsely branching siphons are regarded as ancestral thallus anatomy in siphonous algae (Verbruggen et al., 2009). Although the Omdraaivlei Neoarchean microfossils support such claims, their preservation is too fragmentary for incontrovertible conclusions.

As shown above, many morphological and mineralogical features of the tubular structures found in the Omdraaivlei stromatolites are akin to modern taxa of siphonous algae. A petrographic thin section however, only exhibits a 30 to 100 µm thick section of a microfossil and the different planes of focus are often insufficient to judge the three-dimensional morphology of structures (Schopf and Kudryavtsev, 2012). Therefore, beside micro-tomographic sectioning (Fig. 3F-K, Suppl. movie) for three dimensional examination of the tubular morphology and other anatomical details of the Omdraaivlei microfossils, small cubes were cut from the same rock samples as the thin sections and macerated with 40% hydrofluoric acid (HF). The residua from the dissolved rock samples yielded numerous very brittle fragments of 3D-preserved translucent mineralic-carbonaceous tubes (Figs. 10, 11) corresponding in size, shape and elemental composition with the tubular mineral objects

visible in thin-sections. Most of them showed only simple non-septated, tube-like morphologies, but a few displayed traits permitting indeed a direct comparison with thalli of modern green algae of the order Bryopsidales (class Ulvophyta). These common in modern, particularly tropical seas microalgae are regarded as a core group of green thallophytes (Lam and Zechman, 2006). They have biphasic heteromorphic life-history – a gametophytic generation alternating with a sporophytic generation (Morabito et al., 2003). As shown in Fig. 10, some of the traits observed in the best preserved macerated specimens are characteristic for modern gametophytic generation like terminal branches, gametangia-like structures, or propagation buds. An example of modern analog of the Omdraaivlei gametangium-like structure shown in Fig. 10F is presented in Fig. 10G, whereas thinner, thread-like thalli with characteristic bulging (Fig. 10H, I) can be interpreted as analogs of thalli of modern sporophytic generation (Neumann, 1969; Burr and West, 1970; Chang et al., 2003; Ye et al., 2010). Sparsely branching siphonous thalli and free-living microthalli, and elongate, simple thread-like tubules that could have developed from germinated spores (protonema) (Neumann, 1969; Morabito et al., 2003) were also recognized in the macerated material (Fig. 10J, K). Due to the strong fragmentation of the thalli recovered by maceration, it is unfortunately not possible to apprise whether they belong to one algal taxon or represent a mixture of fragments of several siphonous taxa.

Weak C-signals obtained from SEM-EDS spectra of HF-macerated thalli confirm the presence of carbonaceous material as also documented by NanoSIMS analyses. Traces of Si, K, Al, Ca, Fe, Cl visible in the SEM-EDS spectra may represent remains of the thalli permineralizing silicate phases with possible trace admixture of calcium carbonate (Fig. 11).

Siphonous algae are well documented in the fossil record. Their hitherto oldest organically preserved representatives (*Proterocladus*), ascribed to siphonocladaleans, have been found in Middle and Late Proterozoic marine strata of Spitsbergen (Butterfield et al., 1994; Butterfield,

2004, 2015). Since at least the Neoproterozoic, siphonous algae were common components of shallow-marine biota, their calcified members even achieved a rock-building status in many Phanerozoic geological formations (Riding, 1991). Today, they are represented by a great variety of forms, many with complex thalli, and belong to the most common and ecologically dominant groups of organisms known from tropical marine habitats (Vroom et al., 2006).

5.2. Arguments for exclusion of filamentous cyanobacteria as analogs

As mentioned above, the brownish, non-segmented, C-rich, Fe-Mg aluminosilicate strands observable in thin-sections in the interiors of many Omdraaivlei microfossils (Figs. 2-4, 12B, C) which most probably represent permineralized kerogenous residues of the cell content (cytoplasm) are critical for establishing the bio-affiliation of the tubular objects. These strands, running often continuously from the elongated axial stipes into the dichotomous and trichotomous terminal branches (Figs. 2E, F, 12B, C) represent characteristic bipolar tree- or bush-like body plan, which together with the gametangia-like reproductive structures are important traits clearly discriminating these microfossils from some branching and mineralizing filamentous cyanobacteria. At first glance, these could be, particularly when observed in rock matrix in thin-sections, be considered as analogs of the Omdraaivlei microfossils, particularly when observed in rock matrix in thin-sections (Fig. 12E). Cyanobacterial filaments however, are always built of uni- or multiserially arranged lines of cells forming distinctly regularly segmented structures (Fig. 12F, G) and display very different modes of branching which distinguish them from the mostly feather-like siphonous thallus organization (Figs. 3D, E; 12C), as visible under micro-CT (see supplementary material) and in macerates. Cyanobacterial filaments are averagely one order of magnitude smaller than the tubes of Omdraaivlei microfossils and thalli of modern ‘hair algae’. Filamentous cyanobacteria often show along the cell lines (trichomes) the presence of

specialized reproductive and nutritional structures (akinetes and heterocysts) perturbating the continuity of the normal cell lines (trichomes). Such perturbations were not observed yet in the Omdraaivlei microfossils along the continuous C-rich internal strands interpreted as remains of cell content. Finally, filamentous cyanobacteria seem to be also eliminated as potential analogs of the ~ 2.8-2.7 Ga Omdraaivlei tubular fossils by the results of recent phylogenomic studies showing that such cyanobacterial morphotypes had not exist before 2.2 Ga (Blank and Sánchez-Baracaldo, 2010).

6. Discussion

Accepting the siphonous microalgae affinity of the Omdraaivlei tubular microfossils, the thick mineral envelopes can be explained as probably largely the product of an association between algae and bacteria (Lachnit et al., 2000). Such alliances are known in living siphonous algae and may be beneficial or detrimental for both parties. The bacteria reside either on the surface or within the algal cells (Hollants et al., 2011). Most algae, including siphonous varieties, excrete extracellular polymeric substances on their cell surface (Percival and McDowell, 1981; Ciancia et al., 2012). These excreta are densely settled and utilized by a great variety of heterotrophic bacteria (Lachnit et al., 2000; Goecke et al., 2010; Hollants et al., 2010, 2012). Depending on the hydrochemistry of the environment (particularly pH and the load of metals), the concerted metabolic activity of the algae and of their bacterial settlers changing pH and alkalinity in their proximity, may cause precipitation of various mineral phases. In siphonous algae, calcium carbonate is usually precipitated in such a way on or within the polysaccharide-rich extracellular sheaths, as in many ulvacean and vaucheriacean taxa thriving in alkaline and calcium carbonate oversaturated marine, lacustrine and fluvial

environments (Freytet and Verrecchia, 1998; Golubic et al., 2008; Gradziński, 2010). In the case of the purported Omdraaivlei siphonous microalgae, the lacustrine habitat located in a volcanic setting (Altermann and Lehnhardt, 2012) was probably characterized by circum-neutral pH and less alkaline hydrochemistry (Altermann et al., 2009; Bristow and Milliken, 2011). It seems that such an environment was apparently prone for *in vivo* or early diagenetic precipitation of such aluminosilicate mineral phase as chamosite on, or in the polysaccharide sheaths covering the algae, and of muscovite in the decaying cell content (Figs. 7, 8). Chamosite and muscovite may occur in natural environments as authigenic aluminosilicates. They have been observed in close association with bacteria and microalgae over a range of chemical conditions. Experimental studies have shown (Ferris et al., 1986; Konhauser et al., 1993; Schultze-Lam et al., 1995; Fortin and Beveridge, 1997; Fortin et al., 1997; Konhauser and Urrutia, 1999) that biologically formed chamosite and chamositic clays start to precipitate as amorphous or poorly crystalline phases which, with time, converse continuously to more crystalline forms. The highly variable morphology of the chamosite forming the mineral coatings on the alleged Omdraaivlei microalgae, from microgranules to almost idiomorphic crystals (Figs.2-4) confirms these observations. The *in vivo* or very early post mortem precipitation of the aluminosilicate coatings on the Omdraaivlei algae was most probably the critical factor responsible for their unique 3-D preservation by making the cell wall resistant to lytic processes and the thalli stiff to compaction. Both chamosite and muscovite are mineral phases preferring lower oxygen fugacity and circum-neutral pH in the ambience, during formation (Harder, 1978; Merino et al., 1989). Their association with the Omdraaivlei microalgae-like organisms may therefore be an indirect evidence for their existence in dysoxic or at least not highly oxygenated environment. Generally, precipitation of metal silicates and oxides by various strains of free-living heterotrophic bacteria, cyanobacteria and diminutive green algae is a well-known phenomenon, particularly in metal-loaded, weakly

acidic to circum-neutral environments (e.g., West et al., 1980; Steinberg and Klee, 1984; Köhler et al., 1994; Konhauser et al., 1994; Urrutia and Beveridge, 1994; Tazaki, 1997; Bischoff, 1997; Konhauser and Urrutia, 1999).

Interestingly, the high Ti signals obtained from SEM-EDS spectra and micro-Raman of the rods and granules exposed by HF-etching of the mineral coatings of Omdraaivlei microfossils (Fig. 9C-E) may indicate an uptake of Ti either post mortem by particles of degraded algal mucus sheaths or *in vivo* by some of the mucus-associated microbes and formation of titanium biominerals (here identified by micro-Raman as mixture of anatase and rutile). Titanium is known to be sub-toxic or toxic for many microorganisms and can be neutralized through complexation by their extracellular polymeric substances (Glamoclija et al., 2009).

NanoSIMS generated elemental maps of the Omdraaivlei tubular microfossils exhibit clear relationships among carbon, nitrogen and sulfur, similar to those shown in organically preserved filamentous and spheroidal microfossils from the 0.85 Ga Bitter Springs Formation of Australia (Oehler et al., 2010). The sizes and shapes of the patchily distributed "biogenic" elements in the NanoSIMS maps of the tubular microfossils correspond also to the SEM images of the Ti-rich minute objects and may be an argument for their biogenicity (Oehler et al., 2006; Schopf et al., 2007).

The exceptional preservation of the described microalgae-like microfossils may have been the result of *in vivo* mineralization and fast burial in the lacustrine-volcanic depositional environment (Altermann and Lenhardt, 2012). Because of lack of (bio-)degradation of resistant components in cell walls, the fossilization potential of non-mineralized thalli of siphonalean algae is very low. Fossil remains of organic components of thalli are mostly known from carbonaceous impressions on bedding surfaces of shales. Extremely rare, 3D findings of whole organic thalli of calcareous siphonaleans preserved, like some of the

Omdraaivlei thalli, due to very early silicification of the calcareous envelops of thalli, were described from marine Ordovician limestone by Kozłowski and Kaźmierczak (1968a, b). The high fragmentation of the studied microfossils and their co-occurrence with the fine volcaniclastic sediment incorporated in the stromatolitic laminae suggest that the alleged microalgae were probably not directly associated with the stromatolite–forming microbial mats during life-time, but episodically delivered by stormy winds or floods, as debris from adjacent areas to the stromatolite-sustaining lacustrine environment.

7. Conclusions

The mineralized tubular microfossils from the Neoarchean Omdraaivlei Formation seem to represent the earliest well-preserved microfossils with body organization characteristic for eukaryotic siphonalean organisms. Morphological and mineralogical features, along with the presence and mode of distribution of carbonaceous material in the walls and interiors of the tubular structures, indicate unmistakably their biogenicity. The anatomical organization of these microfossils is well documented and comparable to siphonous thalli of geologically much younger and modern ulvacean (Chlorophyta) or vaucheriacean (Xanthophyta) microalgae. Their thick mineral coatings indicate an early origin for the bio-induced and/or bio-mediated mineralization processes. Since all siphonous algae are oxygenic organisms and obligate aerobes (Graham et al., 2009), our findings support results of recent research advocating early oxygenation of the atmosphere or at least the existence of “oxygen oases” in the Neoarchean or even earlier environment (Buick, 1992; Crowe et al., 2013; Lyons et al., 2014; Mukhopadhyay et al., 2014; Planavsky et al., 2014; Riding et al., 2014; Satkoski et al., 2015). Our studies also create basis for recalibration of the proposed relaxed molecular clock models for siphonous green algae, currently estimated to Neoproterozoic (Verbruggen et al., 2008). The presence of siphonous microalgae-like fossils in the Neoarchean biosphere

corroborates with morphological (Niklas, 2000) and conceptual (Egel, 2012) models assuming siphonous/coenocytic body plan as one of the earliest cellular systems in the evolution of life. The described microalgae-like fossils are over 1.5 byr older than the oldest known lacustrine eukaryotic fossils (Strother et al., 2011) and demonstrate the importance of non-marine environments in the evolution of early life. The evolutionary advanced character of the Omdraaivlei siphonous body plan is underscored by the presence of such anatomical traits as terminal branches, lateral appendages and reproductive structures (gametangia) characterizing most modern bryopsidalean algae. It is, however, possible that their reproduction could had also proceeded by fragmentation of thalli, which is a common reproductive strategy in some extant siphonous algae (Vroom and Smith, 2003).

Acknowledgements

Supported by the National Science Centre, Poland (grant 2011/01/B/ST10/06479 to J. K) and by the Program of Scientific and Technological Co-operation between the Governments of the Republic of Poland and the Republic of South Africa (to J. K. and W. A.). We appreciate the Europlanet TransNational Access Programme for funding access to NanoSIMS facilities at the Milton Keynes Open University (UK). Cyprian Kulicki and Krzysztof Owocki (Warsaw) helped with SEM-EDS and Cameca microprobe analysis. Katarzyna Janiszewska (Warsaw) kindly prepared the micro-tomograph movie and 2-D slices. Comments and suggestions by the Editor and Reviewer are greatly appreciated. The research was partially supported by the European Union within the European Regional Development Fund, through the Innovative Economy Operational Programme POIG.02.02.00-00-025/09/ supported by NanoFun POIG.02.02.00-00-025/09.

References

Altermann, W., Kazmierczak, J., 2003. Archean microfossils: a reappraisal of early life on Earth. Res. Microbiol. 154, 611-617.

Altermann, W., 2007. Accretion, trapping and binding of sediment in Archean stromatolites – morphological expression of the antiquity of life. Space Sci. Rev. 135, 55-79.

Altermann, W., Lenhardt, N., 2012. The volcano-sedimentary succession of the Archean Sodium Group, Ventersdorp Supergroup, South Africa: Volcanology, sedimentology and geochemistry. Precambr. Res. 214-215, 60-81.

Altermann, W., Böhmer, C., Gitter, F., Heimann, F., Heller, I., Läuchli, B., Putz, C., 2009. Defining biominerals and organominerals. Direct and indirect indicators of life. Discussion. Sedim. Geol. 213, 150-151.

Awramik, S.M., 1992. The oldest records of photosynthesis. Photosynthesis Res. 33, 75-89.

Bischoff, G.C.O., 1997. Sorption of Pb-Cu-Fe by microbially-accumulated aluminosilicate on a siliceous gossan encrusted with beaverite and clinochlore; Nevada Mine, N.S.W., Australia. N. Jb. Geol. Paläont. Abh. 204, 201-220.

Blank, C.E., Sánchez-Baracaldo P., 2010. Timing of morphological and ecological innovations in the Cyanobacteria – A key to understanding the rise in atmospheric oxygen. Geobiology 8, 1-23.

Børgesen, F., 1925. Marine algae from the Canary Islands, especially from Teneriffe and Gran Canaria. I. Chlorophyceae. Kongelige Danske Videnskabernes Selskab, Biol. Meddel. 5, 1-123.

Brasier, M., McLoughlin, N., Green, O., Wacey, D., 2006. A fresh look at the fossil evidence for early Archaean cellular life. Phil. Trans. R. Soc. B, 361, 887-902.

Bristow, T.F.; Milliken, R.E., 2011. Terrestrial perspective on authigenic clay minerals production in ancient Martian lakes. Clays Clay Miner. 59, 339-358.

Buck, S.G., 1980. Stromatolite and ooid deposits within the fluvial and lacustrine sediments of the Precambrian Ventersdorp Supergroup of South Africa. Precambr. Res. 12, 311-330.

Buick, R., 1992. The antiquity of oxygenic photosynthesis: Evidence from stromatolites in sulfate-deficient Archean lakes. Science 255, 74-77.

Buick, R., 2010. Ancient Acritarchs. Nature 463, 885-886.

Burr, F.A., West, J.A., 1970. Light and electron microscope observations on the vegetative and reproductive structures of *Bryopsis hypnoides*. Phycologia 9, 17-37.

Butterfield, N.J., 2004. A vaucheriacean alga from the middle Proterozoic of Spitsbergen: implications for the evolution of Proterozoic eukaryotes and the Cambrian explosion. Paleobiology 30, 231-252.

Butterfield, N.J., Knoll, A.H., Swett, K., 1994. Paleobiology of the Neoproterozoic Svanbergfjellet Formation, Spitsbergen. Fossils & Strata 34, 1-84.

Butterfield, N.J., 2015. Early evolution of the Eukaryota. Palaeontology 58, 5-17.

Chang, J.-S., Daia, C.-F., Chang, J., 2003. Gametangium-like structures as propagation buds in *Codium edule* Silva (Bryopsidales, Chlorophyta). Bot. Mar. 46, 431-437.

Ciancia, M., Alberghina, J., Arata, P.X., Benavides, H., Leliaert, F., Verbruggen, H., Estevez, J.M., 2012. Characterization on cell wall polysaccharides of the coenocytic green seaweed *Bryopsis plumosa* (Bryopsidaceae, Chlorophyta) from the Argentine coast. J. Phycol. 48, 326-335.

Crowe, S.A., Døssing, L.N., Beukes, N.J., Bau, M., Kruger, S.T., Frei, R., Canfield, D.E., 2013. Atmospheric oxygenation three billion years ago. Nature 501, 535-538.

Dickerson, R.E., 1971. The structure of cytochrome c and the rates of molecular evolution. J. Mol. Evol. 1, 26-45.

Douzery, E.J.P., Snell, E.A., Bapteste, E., Delsuc, F., Philippe, H., 2004. The timing of eukaryotic evolution: Does a relaxed molecular clock reconcile proteins and fossils? Proc. Natl Acad. Sci. USA 101,15386-15391.

Ducker, S.C., 1967. The genus *Chlorodesmis* (Chlorophyta) in the Indo-Pacific region. Nova Hedwigia 13, 145-182.

Eme, L., Sharpe, S.C., Brown, M.W., Roger, A.J., 2014. On the age of eukaryotes: Evaluating evidence from fossils and molecular clocks. Cold Spring Harb. Perspect. Biol. 6:a016139.

Egel, R., 2012. Primal eukariogenesis: On the communal nature of precellular states, ancestral to modern life. Life 2, 170-212.

Feng, D.F., Cho, G., Doolittle, R.F., 1997. Determining divergence times with a protein clock: Update and reevaluation. Proc. Natl. Acad. Sci. USA 94, 13028-13033.

Ferris, F.G., Beveridge, T.J., Fyfe, W.S., 1986. Iron-silica crystallite nucleation by bacteria in a geothermal sediment. Nature 320, 609-611.

Fortin, D., Beveridge, T.J., 1997. Role of the bacterium, *Thiobacillus*, in the formation of silicates in acidic mine tailings. Chem. Geol. 141, 235-250.

Fortin, D., Ferris, F.G., Beveridge, T.J., 1997. Surface-mediated mineral development by bacteria. In: Banfield J.F., Nealson, K.H. (Eds.), Geomicrobiology: Interactions Between Microbes and Minerals, Rev. Miner. 35, 161-180.

French, K.L., Hallman, C., Hope, J.M., Schoon, P.L., Zumberge, J.A., Hoshino, Y., Peters, C.A., George, S.C., Love, G.D., Brocks, J.J., Buick, R., Summons, R.E., 2015. Reappraisal of hydrocarbon biomarkers in Archean rocks. Proc.Natl. Acad. Sci. USA 112, 5915-5920.

Freytet, P., Verrecchia, E., 1998. Freshwater organisms that build stromatolites: a synopsis of biocrystallization by prokaryotic and eukaryotic algae, Sedimentology 45, 535-563.

Glamoclija, M., Steele, A, Fries, M., Schieber, J., Voytek, M.A., Cockell, C.S., 2009. Association of anatase (TiO_2) and microbes: Unusual fossilization effect or a potential biosignature? Geol. Soc. Amer. Special Publications 336**,** 143-191**.**

Goecke, F., Labes, A., Wiese, J., Imhoff, J.F., 2010. Chemical interactions between marine macroalgae and bacteria. Mar. Ecol. Progr. Ser. 409, 267-300.

Golubić, S., Violante, C., Plenković-Moraj, A., Grgasović, T., 2008. Travertines and calcareous tufa deposits: an insight into diagenesis. Geologia Croatica 61, 363-378.

Gradziński, M., 2010. Factors controlling growth of modern tufa: results of a field experiment. In: Pedley, H.M., Rogerson, M. (Eds.) Tufas and Speleothems: Unravelling the Microbial and Physical Controls.. Geol. Soc. London, Special Publications 336, 143-191.

Graham, L.E., Graham, J.M., Wilcox, L.W., 2009. Algae (2^{nd} ed.). Benjamin Cummings, San Francisco, p. 616.

Grobler, N.J., Van der Westhuizen, W.A., Tordiffe, E.A.W., 1989. The Sodium Group, South Africa Reference Section for late Archaean—early Proterozoic cratonic cover sequences. Austr. J. Earth Sci. 36, 41–64.

Harder, H., 1978. Synthesis of iron layer silicate minerals under natural conditions. Clays Clay Miner. 26, 65-72.

Hedges, S.B., Chen, H., Kumar, S., Wang, D. Y.-C., Thompson, A.S., Watanabe, H., 2001. A genomic timescale for the origin of eukaryotes. BMC Evol. Biol. 1:4.

Hedges, S.B., Blair, J.E., Venturi, M.L., Shoe, J.L., 2004. A molecular time scale of eukaryote evolution and the rise of complex multicellular life. BMC Evol. Biol. 4:2.

Hollants, J.; Leliaert, F.; De Clerck, O.; Willems, A.; 2010. How endo- is endo-? Surface sterilization of delicate samples: *Bryopsis* (Bryopsidales, Chlorophyta) case study. Symbiosis 451, 131-138.

Hollants, J., Leroux, O., Leliaert, F., Decleyre, H., De Clerck, O., Willems, A., 2011. Who is in there? Exploration of endophytic bacteria within the siphonous green seaweed *Bryopsis* (Bryopsidales, Chlorophyta). PLoS One 6(10), e26458.

Hollants, J.; Leliaert, F.; De Clerck, O.; Willems, A., 2012. What we can learn from sushi: a review on seaweeds-bacterial associations. FEMS Microbiol. Ecol. 83, 1-16.

Javaux, E.J., Craig, C.P., Bekker, A., 2010. Organic-walled microfossils in 3.2-billion-year-old shallow-marine siliciclastic deposits. Nature 463, 934-938.

Kaplan, D.R., Hagemann, W., 1991. The relationship of the cell and organism in vascular plants. Bioscience 41, 693-703.

Knoll, A.H., 2014. Paleobiological perspectives on early eukaryotic evolution. Cold Spring Harb. Perspect. Biol. 6:a016121.

Knoll, A.H., 2015. Paleobiological perspectives on early microbial evolution. Cold Spring Harb. Perspect. Biol. 7:a018093.

Knoll, A.H., Javaux, E.J., Hewitt, D., Cohen, P., 2006. Eukaryotic organisms in Proterozoic oceans. Philos. Trans. R. Soc. B 361, 1023-1038.

Konhauser, K.O., Urrutia, M.M., 1999. Bacterial clay authigenesis: a common biogeochemical process. Chem. Geol. 161, 399-413.

Konhauser, K.O., Fyfe, W.S., Ferris, F.G., Beveridge, T.J., 1993. Metal sorption and mineral precipitation by bacteria in two Amazonian river systems: Rio Solimões and Rio Negro, Brazil. Geology 21, 1103-1106.

Konhauser, K.O., Schultze-Lam, S., Ferris, F.G., Fyfe, W.S., Longstaffe, F.J., Beveridge, T.J., 1994. Mineral precipitation by epilithic biofilms in the Speed River, Ontario, Canada. Appl. Environ. Microbiol. 60, 549-553.

Köhler, B.; Singer, A.; Stoffers, P., 1994. Biogenic nontronite from marine white smoker chimney. Clays Clay Miner. 42, 689-701.

Kozłowski, R., Kaźmierczak, J., 1968a. On two Ordovician calcareous algae. Acta Palaeont. Polonica 13, 325-346.

Kozłowski, R., Kaźmierczak, J., 1968b. Sur une Algue ordovicienne conservant le thalle organique. C. R. Acad. Sci. Paris Ser. D 266, 2147-2148.

Lachnit, T., Blümel, M., Imhoff, J.F., Wahl, M., 2000. Specific epibacterial communities on macroalgae: phylogeny matters more than habitat. Aquatic Biology 5,181-186.

Lam, D.W., Zechman, F.W., 2006. Phylogenetic analyses of the Bryopsidales (Ulvophyceae, Chlorophyta) based on rubisco subunit gene sequence. J. Phycol. 42, 669-678.

Lyons, T.W., Reinhard, C.T., Planavsky, N.J., 2014. The rise of oxygen in Earth's early ocean and atmosphere. *Nature* 506, 307-315.

Merino, E., Harvey, C., Murray, H.H. (1989) Aqueous-chemical control of the tetrahedral-aluminum content of quartz, halloysite, and other low-temperature silicates. Clays Clay Miner. 37, 135-142.

Morabito, M., De Masi, F., Gargiulo, G., 2003. Life history of two species of *Bryopsis* from the Straits of Messina (Italy). Bocconea 16, 1059-1066.

Mukhopadhyay, J., Crowley, Q.G., Ghosh, S., Ghosh, G., Chakrabarti, K., Misra, B., Heron, K., Bose, S., 2014. Oxygenation of the Archean atmosphere: New paleosol constraints from eastern India. Geology 42, 923-926.

Neumann, K., 1969. Protonema mit Riesenkern bei der siphonalen Grünalge *Bryopsis hypnoides* und weitere cytologische Befunde. Helgoländer Wissenschaft. Meeresuntersuch. 19, 45-57.

Niklas, K.J. (2000) The evolution of plant body plans—A biomechanical perspective. Ann. Bot. 85, 411-438.

Nisbet, E.G., Sleep, N.H., 2001. The habitat and nature of early life. Nature 409, 1083-1091.

Oehler, D.Z., Robert, F., Walter, M.R., Sugitani, K., Meibom, A., Mostefaoui, S., Gibson, E.K., 2010. Diversity in the Archean biosphere: New insights from NanoSIMS. Astrobiology 10**,** 413-424.

Oehler, D.Z.; Robert, F.; Mostefaoui, S.; Meibom, A.; Selo, M.; McKay, D.S., 2006. Chemical mapping of Proterozoic organic matter at submicron spatial resolution. Astrobiology 6, 838-850.

Parfrey, L.W., Lahr, D.J.G., Knoll, A.H., Katz, L.A., 2011. Estimating the timing of early eukaryotic diversification with multigene molecular clocks. Proc. Natl. Acad. Sci. USA 108, 13624-13629.

Percival, E., McDowell, R.H., 1981. Algal walls. Composition and biosynthesis. In: Tanner, W., Loewus, F.A. (Eds.), Encyclopedia of Plant Physiology vol. 13B. Springer, Berlin, pp. 277-316.

Planavsky, N.J., Asael, D., Hofmann, A., Reinhard, C.T., Lalonde, S.V., Knudsen, A., Wang, X., Ossa, F.O., Pecoits, E., Smith, A.J.B., Beukes, N.J., Bekker, A., Johnson, T.M., Konhauser, K.O., Lyons, T.W., Rouxel, O.J., 2014. Evidence for oxygenic photosynthesis half a billion years before the Great Oxidation Event. Nat. Geosci. 7, 283-286.

Pulquério, M.J.F., Nichols, R.A., 2007. Dates from the molecular clock: how wrong can we be? Trends Ecol. Evol. 22**,** 180-184.

Rasmussen, B., Fletcher, I.R., Brocks, J.J., 2008. Reassessing the first appearance of eukaryotes and cyanobacteria. Nature 455, 1101-1105.

Riding, R., (Ed.), 1991. Calcareous Algae and Stromatolites. Springer, Berlin, p. 571.

Riding, R., Fralick, P., Liang, L., 2014. Identification of an Archean marine oxygen oasis. Precambr.Res. 251, 232-237.

Roger, A.J., Hug, L.A., 2011. The origin and diversification of eukaryotes: problems with molecular phylogenetics and molecular clock estimation. Philos. Trans. R. Soc. B 361, 1039-1054.

Satkoski, A.M., Beukes, N.J., Li, W., Beard, B.L., Johnson, C.M. 2015. A redox-stratified ocean 3.2 billion years ago. Earth Planet. Sci. Lett. 430, 43-53.

Schopf, J.W., Kudryavtsev, A.B., Czaja, D., Tripathi, A.B., 2007. Evidence of Archean life: stromatolites and microfossils. Precambr. Res. 158, 141–155.

Schopf, J.W., Kudryavtsev, A.B., 2012. Biogenicity of Earth's earliest fossils: A resolution of the controversy. Gondwana Res. 22, 761–771.

Schultze-Lam, S., Urrutia, M.M., Beveridge, T.J., (1995) Metal and silicate sorption and subsequent mineral formation on bacterial surfaces: subsurface implications. In: Allen, H.E. (Ed.), Metal Contaminated Aquatic Sediments. Ann Arbor Press, Chelsea, pp. 111–147.

Steinberg, C., Klee, R., 1984. Zur Chemie von *Trachelomonas*-Loricae. *Archiv Protistenk.* 128, 283-294.

Strother, P.K., Battison, L., Brasier, M.D., Wellman, C.H., 2011. Earth's earliest non-marine eukaryotes. Nature 473, 505-509.

Tazaki, K., 1997. Biomineralization of layer silicates and hydrated Fe/Mn in microbial mats: an electron microscopical study. Clays Clay Miner. 45, 203-212.

Urrutia, M.M., Beveridge, T.J., 1994. Formation of fine-grained metal and silicate precipitates on a bacterial surface (*Bacillus subtilis*). Chem. Geol. 116, 261–280.

Van der Westhuizen, W.A., de Bruiyn, H., Meintjes, P.G. 1991. The Ventersdorp Supergroup: an overview. J. African Earth Sci. 13, 83–105.

Verbruggen, H., Schils, T., 2012. *Rhipilia coppejansii*, a new coral reef-associated species from Guam (Bryopsidales, Chlorophyta). J. Phycol. 48, 1090-1098.

Verbruggen, H., Vlaeminck, C., Sauvage, T., Sherwood ,A.R., Leliaert, F., De Clerck, O., 2009. Phylogenetic analysis of *Pseudochlorodesmis* strains reveals cryptic diversity above the family level in the siphonous green algae (Bryopsidales, Chlorophyta). J. Phycol. 45, 726-731.

Verbruggen, H., Ashworth, M.; LoDuca, S.T.; Vlaeminck, C.; Cocquyt, E.; Sauvage, T.; Zechman, F.W.; Littler, D.S.; Littler, M.M.; Leliaert, F.; De Clerck, O., 2008. A multi-locus time calibrated phylogeny of the siphonous green algae. Mol. Phyl. Evol. 50, 642-653.

Vroom, P.S., Smith, C.M., 2003 Life without cells. Biologist 50, 222-226.

Vroom, P.S., Page, K.N., Kenyon, J.C., Brainard, R.E., 2006. Algae-dominated reefs. American Scientist 94, 430-437.

Waldbauer, J.R., Sherman, L.S., Summner, D.Y., Summons, R.E., 2009. Late Archean molecular fossils from the Transvaal Supergroup record the antiquity of microbial diversity and aerobiosis. Precambr. Res. 169, 28-47.

West, L.K., Walne, P.L., Bentley, J., 1980. *Trachelomonas hispida* var. *coronata* (Euglenophyceae. III. Envelope elemental composition and mineralization. J. Phycol. 16, 582-591.

Ye, N., Wang, H., Gao, Z., Wang, G., 2010. Laboratory studies on vegetative regeneration of the gametophyte of *Bryopsis hypnoides* Lamouroux (Chlorophyta, Bryopsidales). Afr. J. Biotech. 9, 1266-1273.

Yoder, A.D., 2013. Fossils versus clocks. Science 339, 656-658.

Figure Captions

Fig. 1. Geographic and stratigraphic setting of the tubular microfossils-bearing strata. (A) Location (arrow) of the outcrop of the Neoarchean Omdraaivlei Formation deposits (Sodium Group, Ventersdorp Supergroup, Kaapvaal Craton, South Africa). (B) Fragment of lithological profile of the middle Omdraaivlei Formation; black arrows denote the stromatolitic horizons with remains of the tubular microfossils and red arrow head marks the main stromatolite horizon from which best preserved specimens of the microfossils were collected.

Fig. 2. Stromatolites from the Neoarchean Omdraaivlei Formation with entrapped fragments of tubular microfossils. (A) Stratiform stromatolite from the horizon enclosing best preserved remnants of the tubular microfossils (bed 11 – see profile in Fig. 1). (B) Asymmetrical ripple marks at the top of the same stromatolite horizon (bed 11) indicate shallow current agitated environment in which the stromatolites accreted and entrapped broken remains of the microfossils inflowing with fine tuffaceous material. (C) Transmitted light micrograph of vertical petrographic thin-section of a tubular microfossils-bearing stromatolite with patches and layers of fine detrital sediment (arrows) and fragments of the microfossils. (D-G) Magnified micrographs of the fragmented microfossils (some arrowed), randomly distributed in chertified volcaniclastic (tuffaceous) sediment trapped and bound between stromatolite laminae. Scale bars: (C), 1 mm; (D), 250 μm; (E, F), 100 μm. All micrographs sample SA-31.

Fig. 3. Examples of siphonous microalgae-like tubular fossils from the Neoarchean Omdraaivlei Formation in optical and X-ray micro-tomographic (μCT) sections. (A-E) Optical micrographs of thin-sections of dichotomously (A and B), trichotomously (C), and feather-like (D and E) branching non-septate structures composed of thick-walled mineral tubes with continuous carbon-rich (kerogenous) band inside. Note the presence of mineral envelopes also in the first and the second order branches. (F-K) Serial tomographic slices taken each at ~6 μm distance. The images show longitudinal plane sections of a stipe-like thallus with terminal branches (see also movie – Suppl. Fig. 1). (L and M) Drawings of non-mineralized modern marine siphonous green microalgae for comparison: *Pseudochlorodesmis furcellata* (L), with similarly simple dichotomous and trichotomous thallus organization, and *Bryopsis corymbosa* (M), with feather-like mode of terminal branching; both from Børgesen

(1925). (A and B) – sample SA-31; (C-K) – sample SA2-178. Scale bars for (A-K) 50 μm; for (L) and (M) 500 μm.

Fig. 4. Optical micrographs of siphonous microalgae-like tubular microfossils from the Neoarchean Omdraaivlei Formation. (A) Elongated fragment of mineralized siphonous thalli-like microfossil in longitudinal axial section. (B) Slightly magnified fragment of thallus in longitudinal section showing the blocky and/or granular character of silicate material forming the coating on the cell wall (arrow). The carbon-enriched, striated internal silicate strand, which fills not entirely the tube interior and can be interpreted as remain of shrunken cell content. (C-D) Cross sections fragments of externally rough mineralized tubular thalli showing smooth internal surface of the crystalline mineral coating delimiting the position of the former cell wall (arrows). The tube mineral coatings are in part composed of blocky silicate crystals, and in part of almost homogenous silicate material with various admixture of fine kerogenous matter. Scale bars: (A), 50 μm; (B-D), 30 μm. All from sample SA-31.

Fig. 5. Analytical data of the tubular microfossils from the Neoarchean Omdraaivlei Formation. (A) Electron probe microanalysis (EPMA) of a fragment of tubular microfossil showed as back-scattered-electron microprobe (BSE) image (left) with numbered arrows indicating location of spots analyzed for elemental composition (right): 1 – cherty background, 2 –tube interior 3 – tube mineral coating. Note the higher content of Fe and Mg in the aluminosilicate from the tube coating, comparing to the Si and K enriched aluminosilicate in the tube interior (sample SA-31). (B) Optical image of a tubular microfossil with arrow indicating the micro-Raman mapping spot; (C) A representative Raman spectrum collected from the same microfossil; D (1351 cm^{-1}) and G-bands (1602 cm^{-1}) correspond to

carbon. (D and E) NanoSIMS element maps of a slightly oblique longitudinal section of two tubular microfossils (at left of both maps are optical images showing spot areas). Color bars indicate intensity of response, with blue being lowest and white being highest. Of importance as biogenicity indicators are patches with high $^{12}C^-$, $^{12}C/^{14}N^-$, and $^{32}S^-$ signals on the maps, which locations conform well with the remains of mineralized rod-like and coccoidal bacteria-like structures shown in Fig. 9A and B. Both from sample SA-31. Scale bars: (A), 50 µm; (B), 40 µm; overview images in (D) and (E), 80 µm; NanoSIMS images, 2 µm.

Fig. 6. Analytical data of the tubular microfossils from the Neoarchean Omdraaivlei Formation. Energy Dispersive Spectroscopy (SEM/EDS) maps showing distribution of elements in a fragment of matrix embedded mineral tubes imaged as SEM/BSE in panel (A). Sample S2-31. Scale bar for all equals 100 µm.

Fig. 7. Analytical data of the tubular microfossils from the Neoarchean Omdraaivlei Formation. SEM/EDS analyses of a fragment of mineralized tube-like microfossil (SEM/BSE at the top) showing different elemental composition of the mineral cell coating and the mineralized internal strand. Two aluminosilicate phases are identified stoichiometrically: one close to Mg chamosite (blue frame on top image) and the other suggestive for muscovite (yellow frame on top image). Sample SA2-178. Scale bar equals 50 µm.

Fig. 8. Mineral components of the tubular microfossils from the Neoarchean Omdraaivlei Formation. Bulk X-ray diffractometry (XRD) of the cherty (quartz) matrix with fragments of the siphonous microfossils in samples SA-31 and SA2-178. The XRD identification of Mg chamosite and muscovite 2M1 in both samples corroborates with the stoichiometrically calculated aluminonosilicate phases measured on the basis of SEM/EDS elemental

composition of the cell wall mineral coating and of the mineralized internal band obtained from thallus fragment in sample SA2-178 (see also Fig. 7).

Fig. 9. HF-etched mineral coatings of tubular microfossils from the Neoarchean Omdraaivlei Formation with embedded Ti-enriched mineral microstructures. (A and B) SEM images of longitudinal sections of HF-etched thick mineral (Al-silicate) coating of Omdraaivlei Fm. microfossils with numerous minute whitish bodies exposed by etching (arrowed). (C and D) Elemental electron dispersive spectra (SEM/EDS) of the same mineral coating; in contrast to the titanium-rich bodies (C), the bulk of the mineral coating shows Al-K-Mg-Fe-silicate composition (D). (E) Raman spectra suggest mixture of anatase and rutile for the titanium-rich objects. Scale bars: (A), 5 μm; (B), 2 μm. Sample SA2-178.

Fig. 10. Fragments of tubular microfossils macerated with HF from silicified stromatolites of the Neoarchean Omdraaivlei Formation, showing anatomical features suggesting affiliation with modern green microalgae from the order Bryopsidales ("hair algae"). (A) Main axis (stipe) of thallus-like microfossil with bunch of terminally located branches. (B) Terminal fragment of dichotomously branching siphon-like tube with fusiform structure enclosing object (arrow) similar to propagation buds occurring in modern siphonous *Codium edule*. (C and D) Fragments of tubes with remains of fusiform structures (arrowed) resembling gametangia of bryopsidalean microalgae. (E) The same specimen as (D) photographed in polarized light to underscore weak permineralization of the tube wall. (F) Fragment of a tube with side branch (white arrow) and gametangium-like structure (black arrow) almost identical with those produced in modern bryopsidalean microalga *Codium fragile* shown for comparison in (G). (H-J) Fragments of broken simple (H) or diverging (J) tubes representing probably remains of sporophytic generation of bryopsidalean-like thalli, often with bulges

characteristic of initial parts of growing sporophyte (I). (K) Closed tubular structure reminiscent of free-floating microthalli known in modern members of bryopsidalean microalgae.

With the exception of (E), all transmitted plain light micrographs. All from sample SA-31. (G) ,[https://www.google.pl/search?q=Bryopsis+gametangia&source=lnms&tbm=isch&sa=X&ved=0CAgQ_AUoAmoVChMI1Pysmp3ZxwIVq55yCh0EDg58&biw=1680&bih=900#imgrc=Pn5Pje83EIuPTM%3A].

Scale bars: (A), 100 μm; (B), 50 μm; (C), 30 μm; (D-G), 20 μm; (H), 100 μm (I-K), 50 μm.

Fig. 11. Tubular microfossils from the Neoarchean Omdraaivlei Formation reminiscent of modern siphonous microalgae. (A-D) Optical micrographs of fragments of HF-macerated tubular microfossils imaged in plain (A and C) and polarized (B and D) light. Polarization reveals traces of permineralization preserved in the macerates. Cw – cell wall, Cc – remains of shrunken and detached from the cell wall epiparietal protoplast. Arrow heads indicate mechanical ruptures in cell walls caused either by maceration procedure (A and C) or early diagenetic degradation processes (?dehydration). (E and F) SEM/EDS spectrum (E) of a fragment of macerated tubular microfossil (F), analyzed on Cu-band and sputtered with Pt, shows the presence of C and elements typical for silicate minerals. Scale bars for all 50 μm. Sample SA2-178.

Fig. 12. Comparison of morphological organization in modern siphonous microalgae and Omdraaivlei siphonous microalgae-like tubular microfossils with that of modern filamentous cyanobacteria. (A) Modern siphonous microalga *Bryopsis salvadoreana* (retrieved from: https://www.google.pl/search?q=bryopsis&tbm=isch&imgil=UZKZq7G4m5LjEM%253A%2

53BZSOpVDvbial_BM%253Bhttp%25253A%25252F%25252Fbiogeodb.stri.si.edu%25252Fbioinformatics%25252Fdfm%25252Fmetas%25252Fview%25252F30993&source=iu&pf=m&fir=UZKZq7G4m5LjEM%253A%252CZSOpVDvbial_BM%252C_&usg=__dI0eMm6fdp3Bpugqm8hpgq5WaJI%3D&biw=1680&bih=928&ved=0ahUKEwjQlKnU0LTMAhXG3CwKHU5UB98QyjcIJg&ei=d7wjV5D9Lca5swHOqJ34DQ#imgrc=J1Cj-uh3nnvzpM%3A) with branching thallus showing distinctly continuous (i.e. not segmented) cell content. (B) Dichotomous (B) and feather-like (C) terminal branching of Omdraaivlei mineralized microalgae-like tubular microfossils in petrographic thin-sections; note the similarly continuous character of the kerogen-rich axial band representing variously shrunken cell content; (D) Magnified axial section of fragment of Omdraaivlei microfossil to show the mineral coating and the continuous shrunken cell content ; sample SA-31. (E) Mode of branching in modern cyanobacterium *Tolypothrix* built of filaments (trichomes) of uniseriate lines of cells (retrieved from: https://www.google.pl/search?q=branching+in+cyanobacteria&biw=1680&bih=928&source=lnms&tbm=isch&sa=X&ved=0ahUKEwid8P-bmLfMAhVmYZoKHYS_AHwQ_AUIBigB#imgrc=pjfQPmu_ksSOcM%3A). (F and G) Optical micrographs of fragments of filaments of modern unsheathed (*Phormidium* – F) and ensheathed (*Anabaena* - G) filamentous cyanobacteria to show the septate character of filaments composed of tightly adhering and linearly arranged short-cylindrical or rounded barrel-shaped cells; note the contrast with the continuous (non-septate) cell content in the modern siphonous microalga (A) and the internal carbonaceous bands representing the remains of the variously shrunken cell content in the Archean tubular (siphonous) microfossils shown in (B) to (D). Scale bars: (A) 100 μm, (B) and (C) 50 μm; (D) and (E) 20 μm; (F) and (G) 10 μm.

Supporting information

1. Micro-tomographic movie of a branching specimen of siphonous microalgae-like tubular microfossil from the ~2.8-2.7 Ga Omdraaivlei Formation of South Africa. Supplemental illustration to the series of slices of the same specimen shown in Fig. 3.

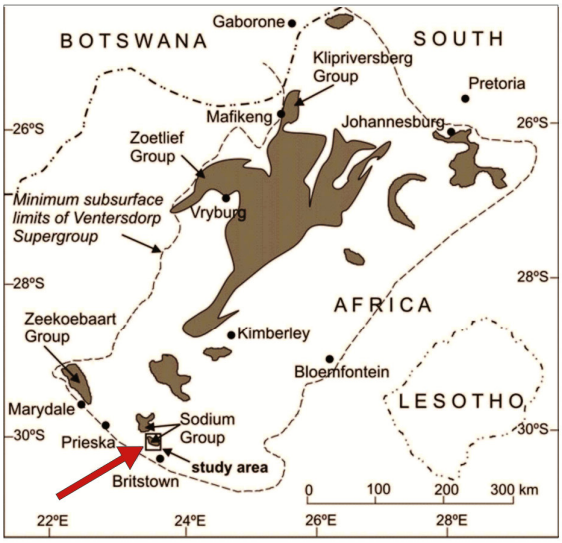

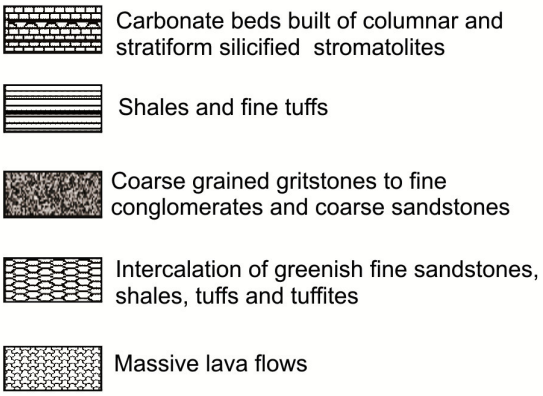

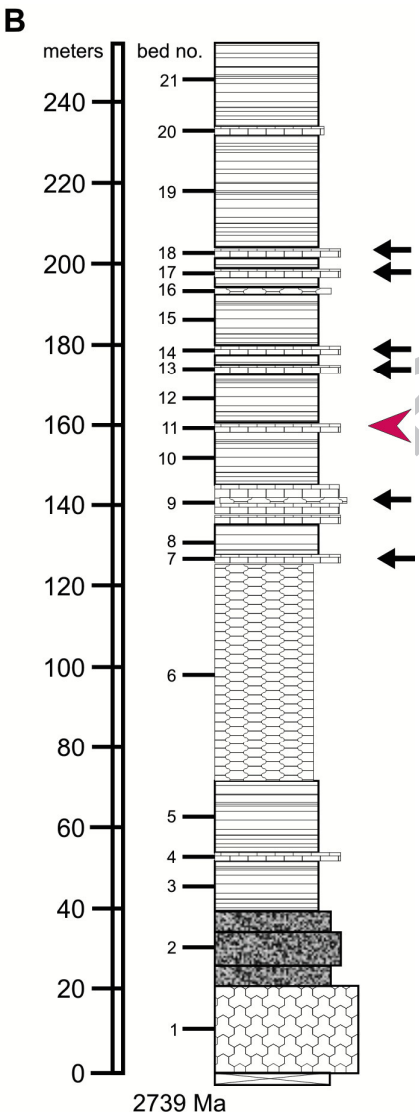

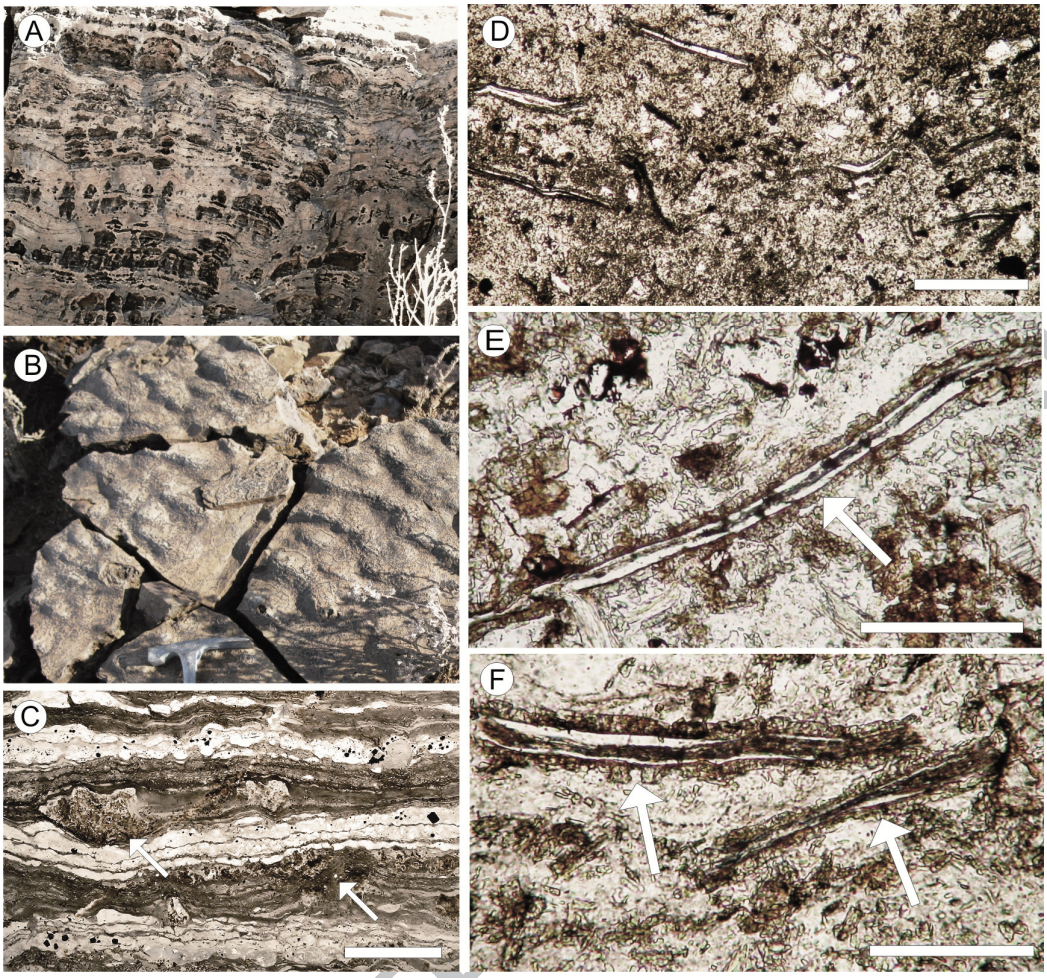

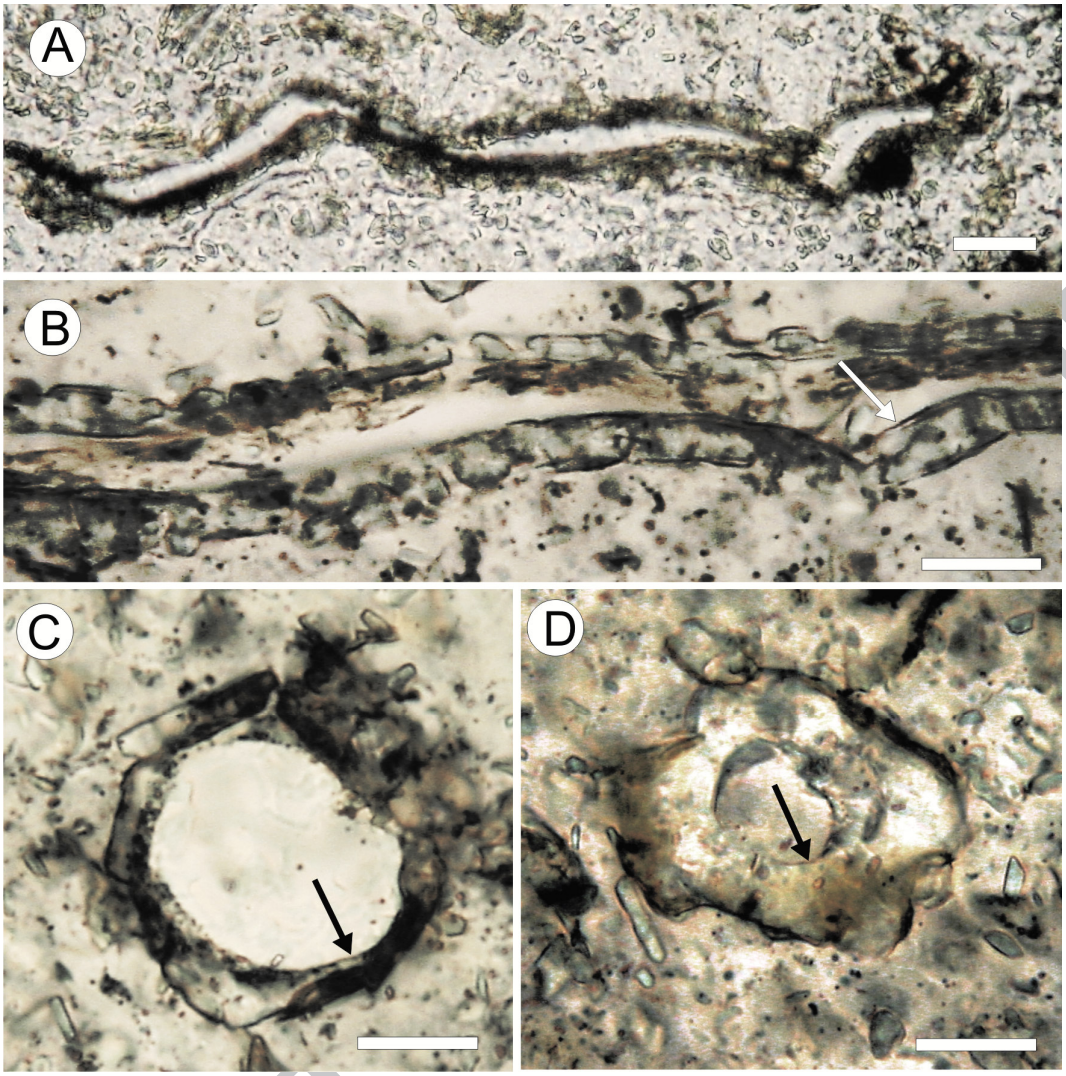

A

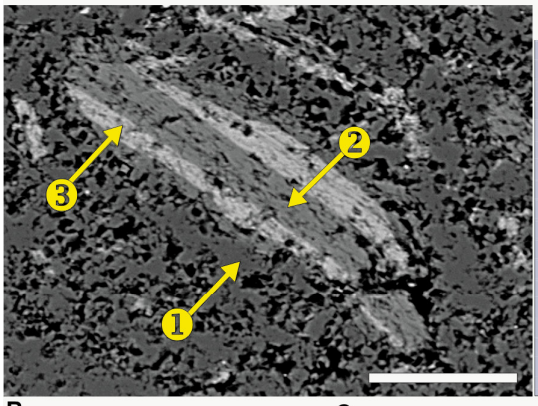

Elements	1	2	3
K	0.000	9.302	0.092
Ca	0.022	0.000	0.000
Ti	1.224	0.459	0.026
Pb	0.004	0.000	0.000
S	0.000	0.000	0.007
P	0.014	0.000	0.005
Mn	0.000	0.074	0.131
Fe	0.557	4.293	24.251
Ni	0.012	0.000	0.016
V	0.372	0.038	0.094
Ba	0.000	0.000	0.000
Na	0.007	0.150	0.016
Si	45.395	22.020	11.330
Mg	0.018	1.076	5.209
Al	0.080	16.445	11.678
O	53.071	44.571	37.293
	100.776	98.428	90.148

B

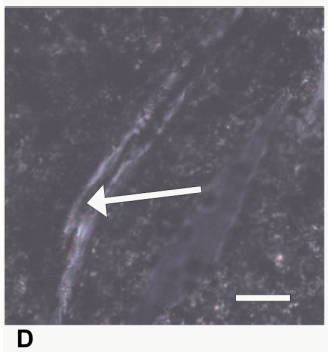

C

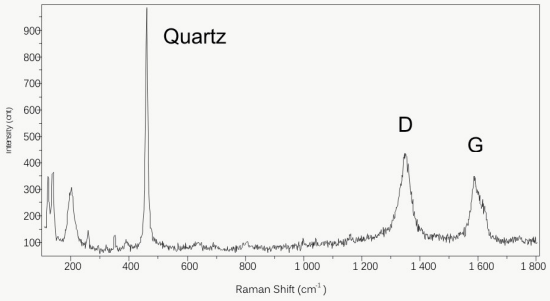

D

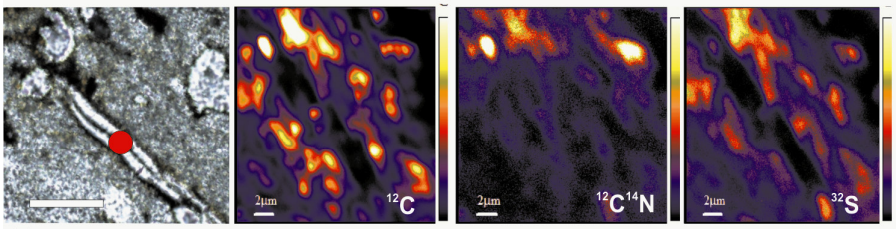

E

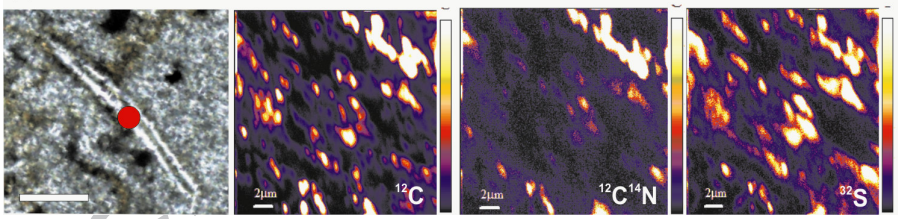

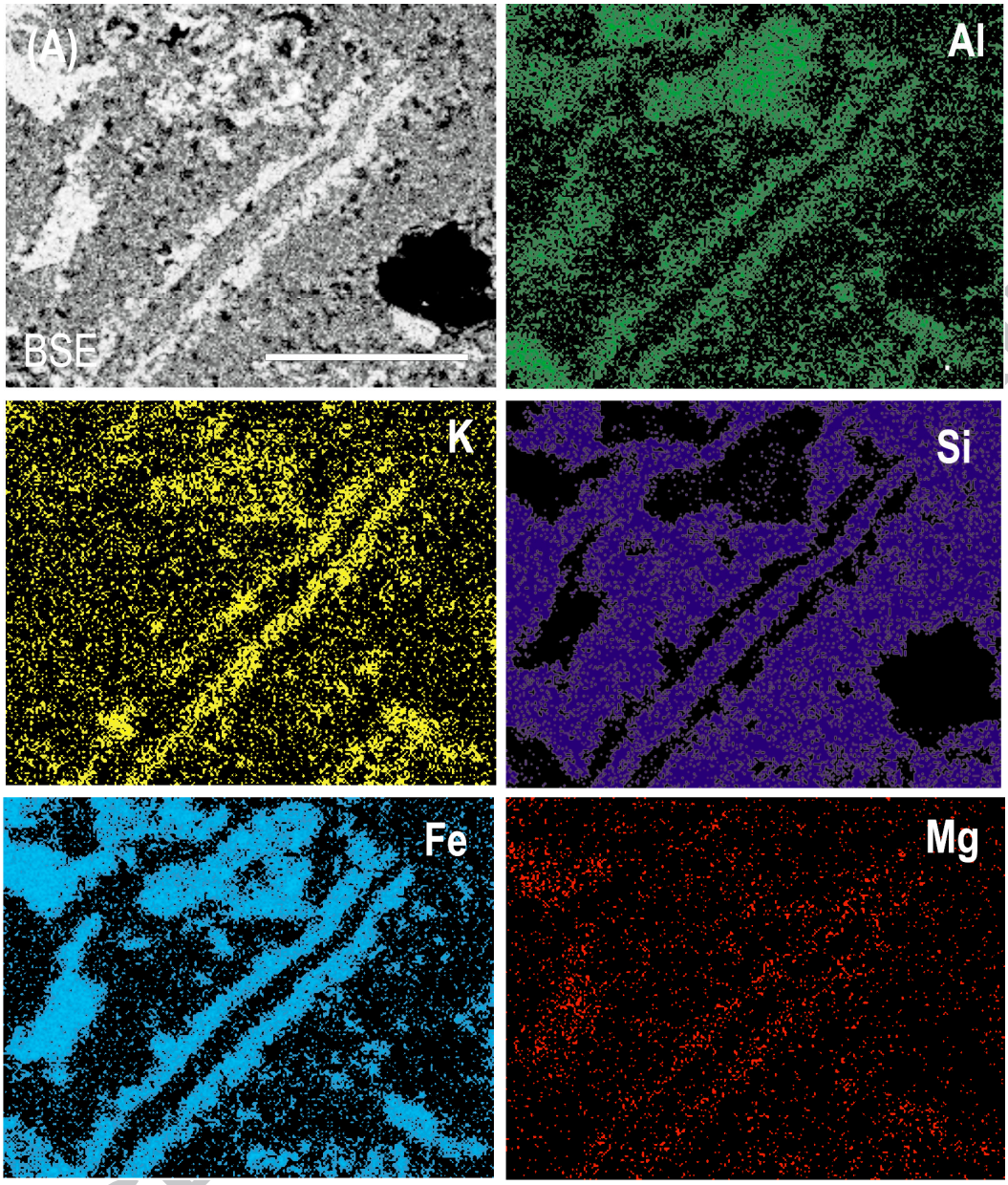

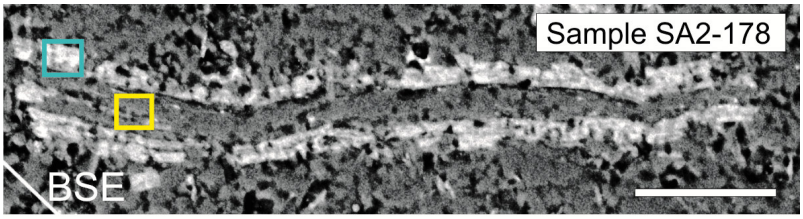
Sample SA2-178
BSE

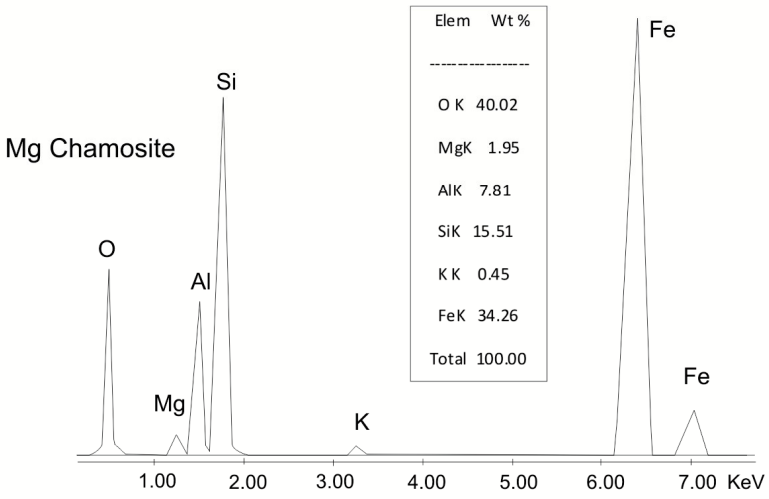
Mg Chamosite
Elem Wt %
O K 40.02
MgK 1.95
AlK 7.81
SiK 15.51
K K 0.45
FeK 34.26
Total 100.00
O
Mg
Al
Si
K
Fe
Fe
1.00
2.00
3.00
4.00
5.00
6.00
7.00 KeV

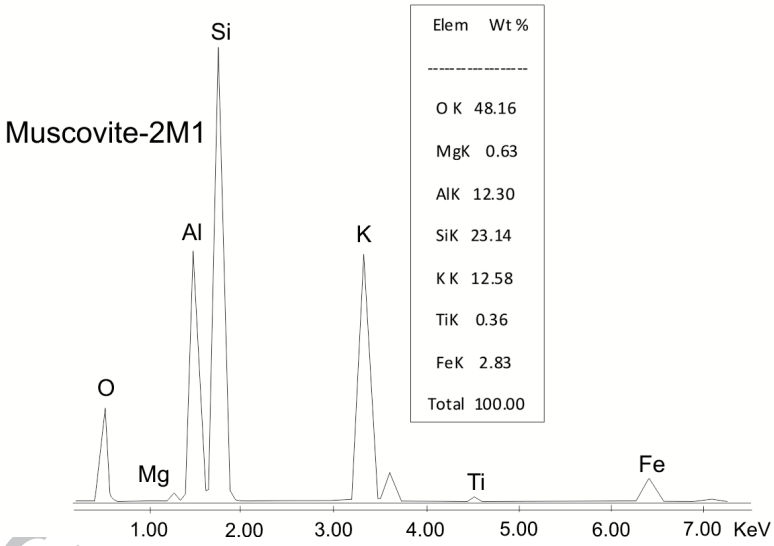
Muscovite-2M1
Elem Wt %
O K 48.16
MgK 0.63
AlK 12.30
SiK 23.14
K K 12.58
TiK 0.36
FeK 2.83
Total 100.00
O
Mg
Al
Si
K
Ti
Fe
1.00
2.00
3.00
4.00
5.00
6.00
7.00 KeV

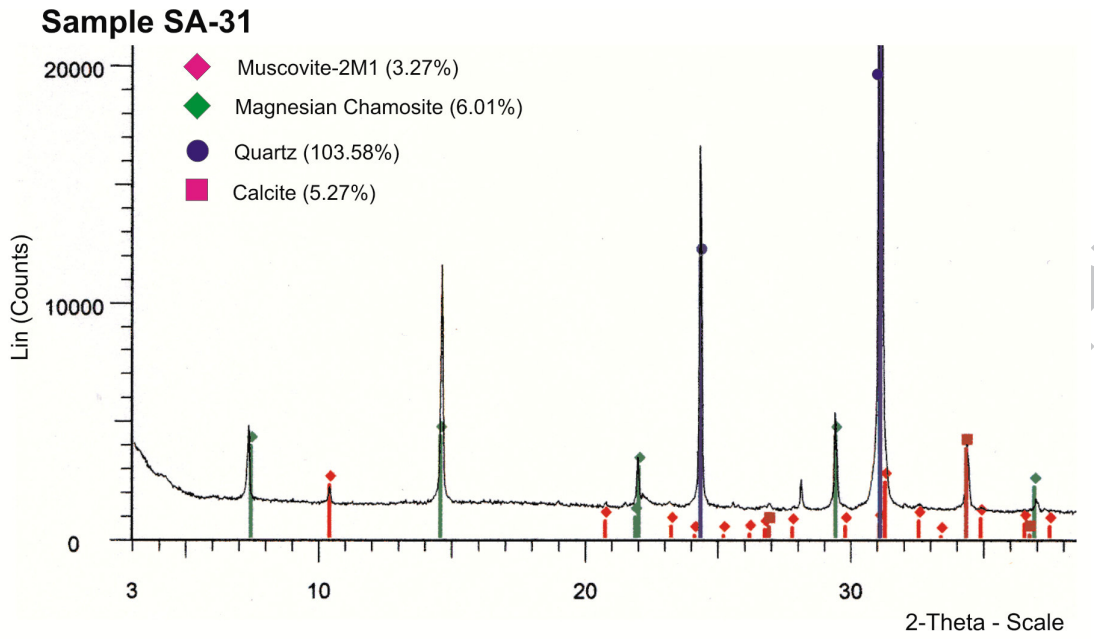

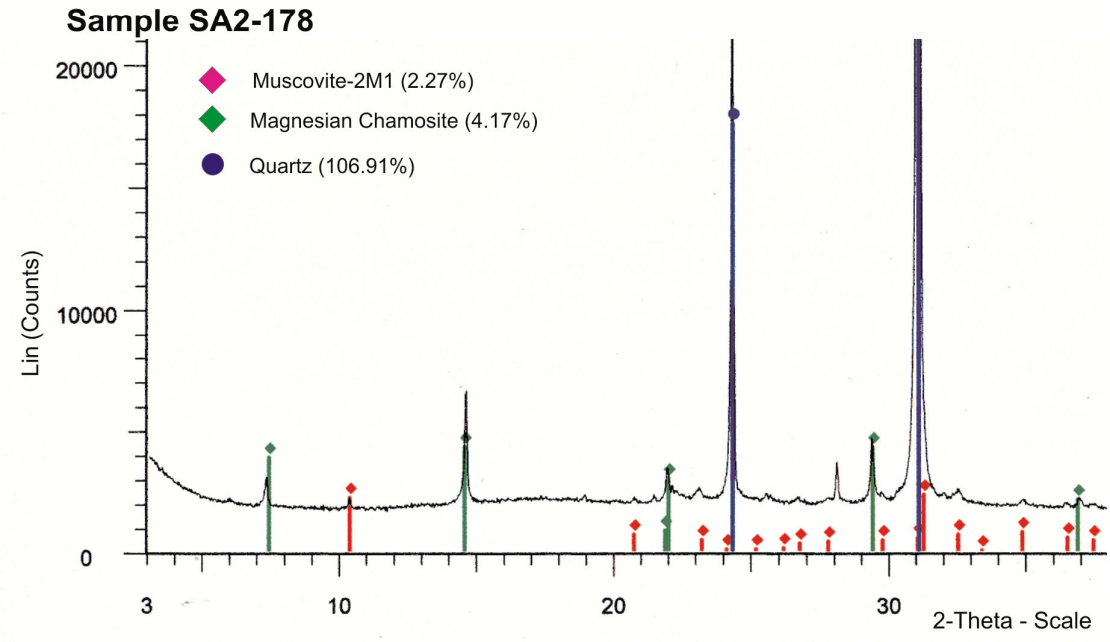

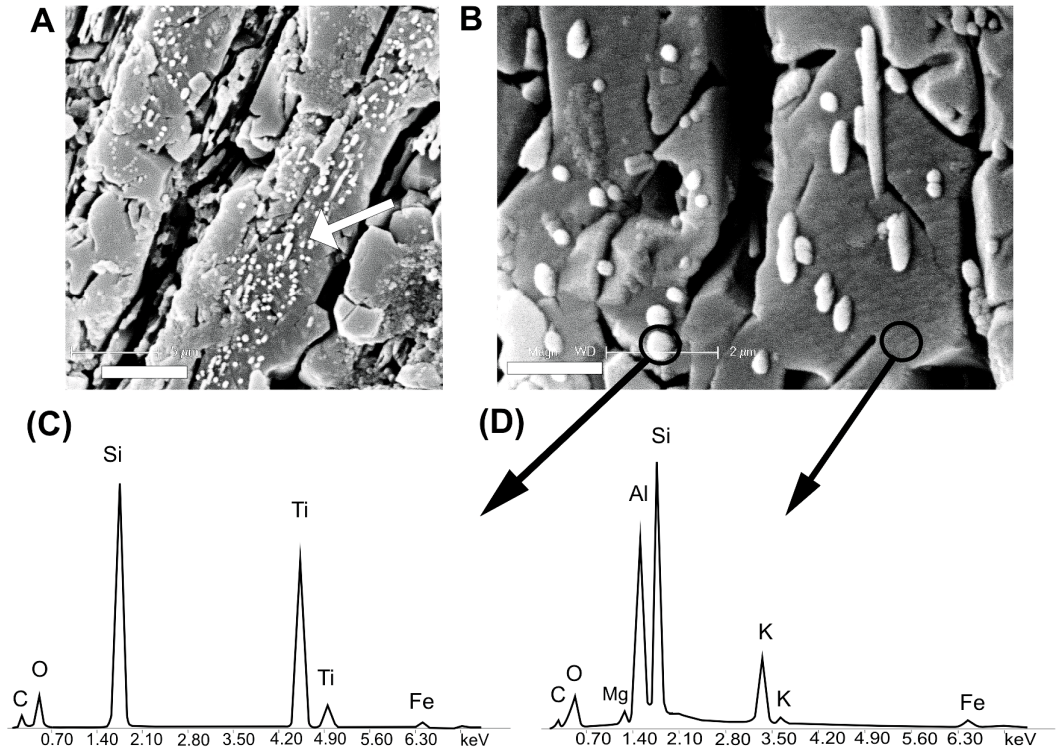

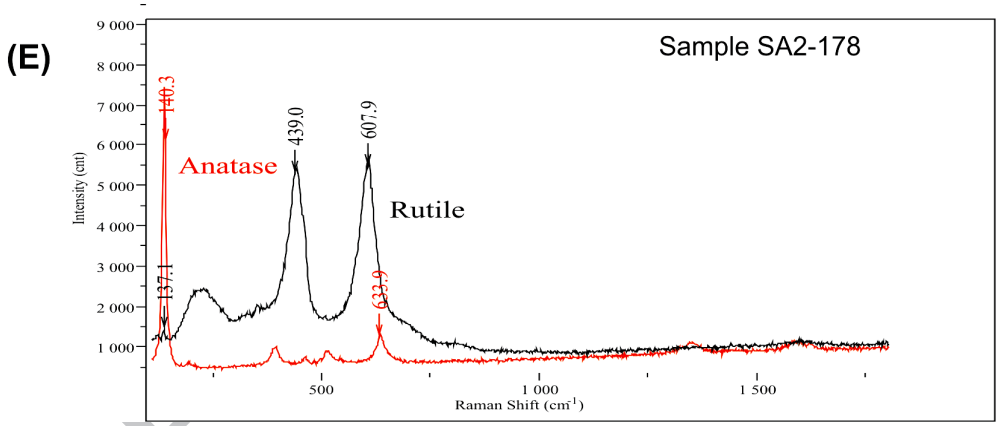

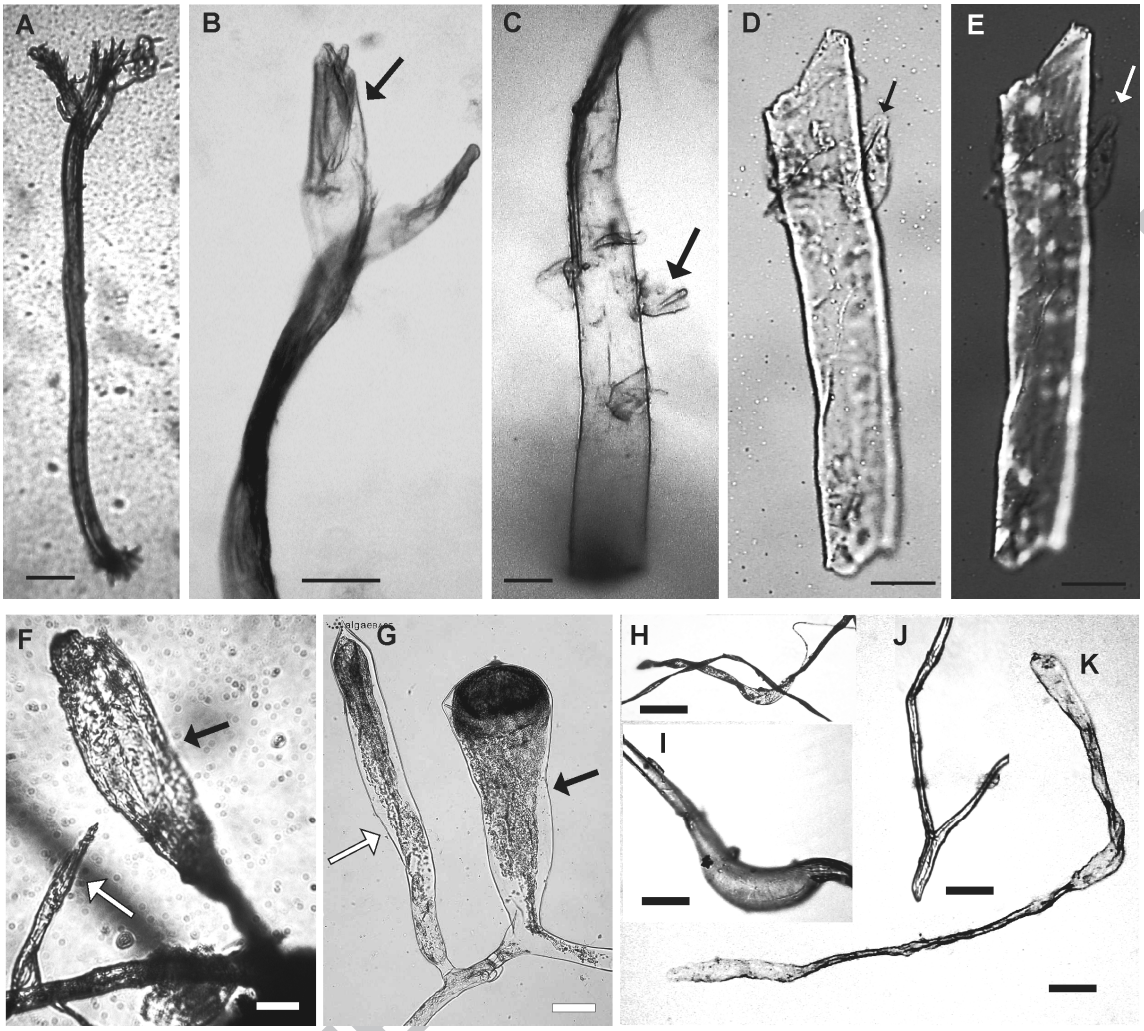

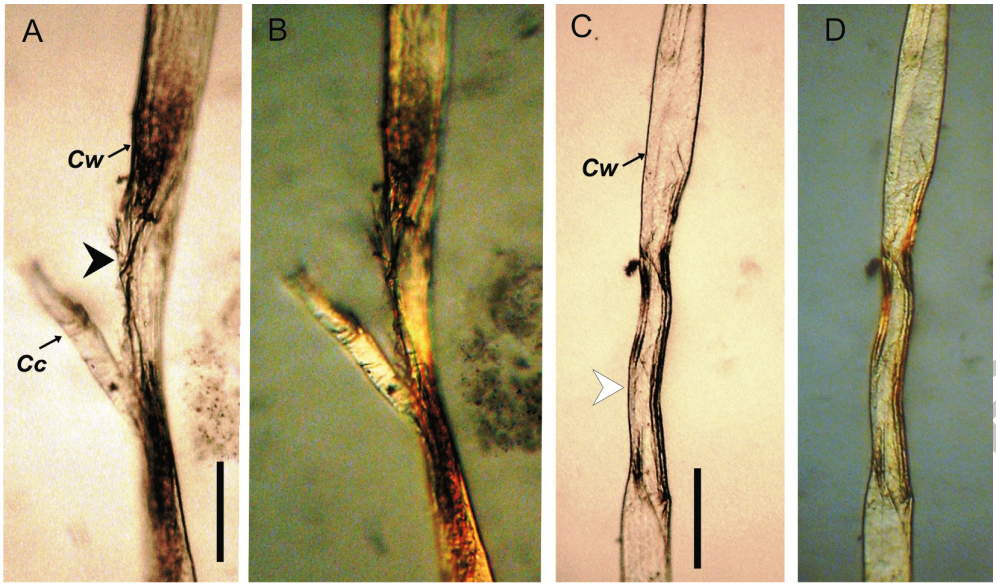

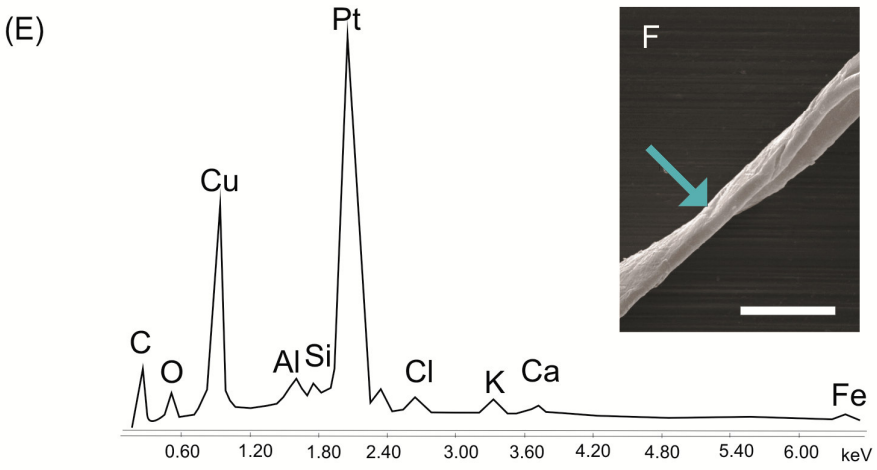

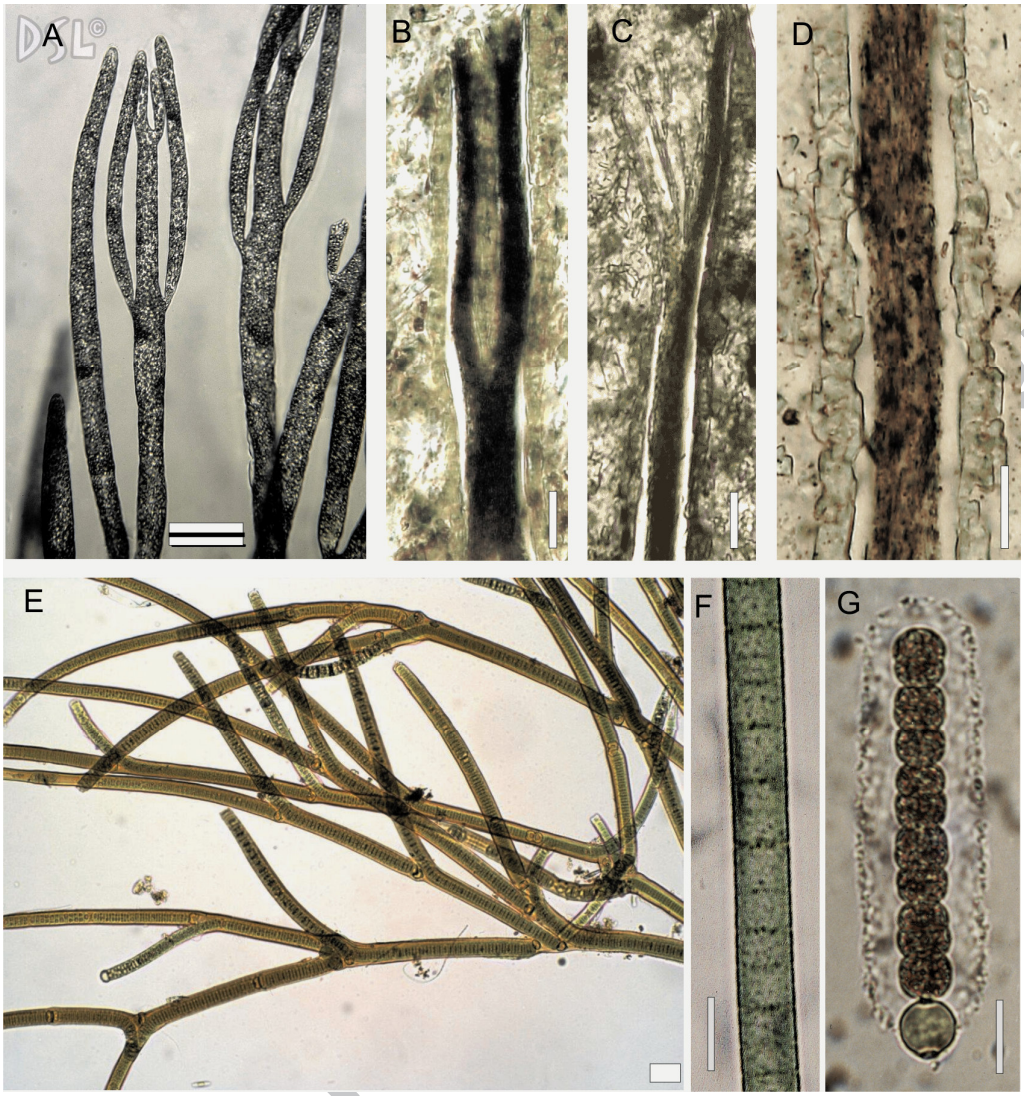

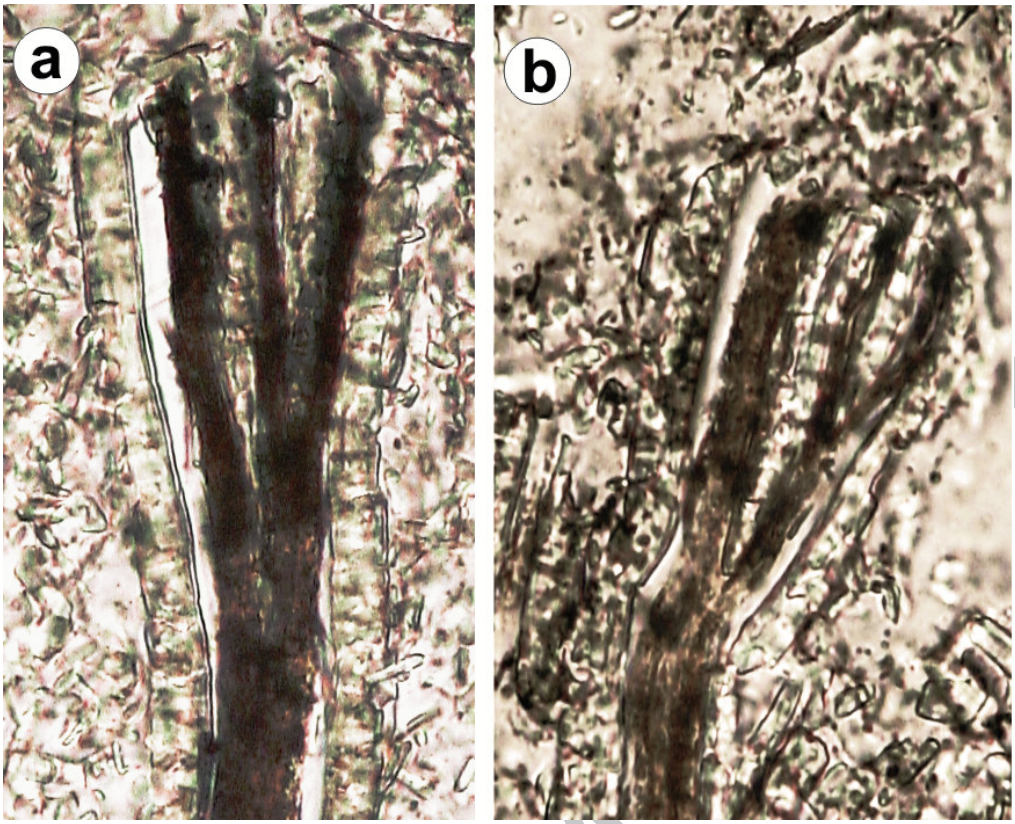

Graphical abstract

Highlights

Neoarchean microbialites from South Africa enclose tubular microfossils

They are reminiscent of modern siphonalean microalgae

These microfossils may represent earliest morphologically preserved eukaryotes